Acta Pharmaceutica Sinica B 2024;14(9):3901−3915

Chinese Pharmaceutical Association
Institute of Materia Medica, Chinese Academy of Medical Sciences

Acta Pharmaceutica Sinica B

www.elsevier.com/locate/apsb
www.sciencedirect.com

ORIGINAL ARTICLE

Abelmoschus manihot polysaccharide fortifies intestinal mucus barrier to alleviate intestinal inflammation by modulating *Akkermansia muciniphila* abundance

Yumeng Wang [a,b,†], Chengxi Li [a,b,†], Jianping Li [a,b,†], Shu Zhang [a,b], Qinyu Zhang [a,b], Jinao Duan [a,b,*], Jianming Guo [a,b,*]

[a]*Jiangsu Collaborative Innovation Center of Chinese Medicinal Resources Industrialization, Nanjing University of Chinese Medicine, Nanjing 210023, China*
[b]*Jiangsu Key Laboratory for High Technology Research of TCM Formulae, Nanjing University of Chinese Medicine, Nanjing 210023, China*

Received 26 March 2024; received in revised form 9 May 2024; accepted 30 May 2024

KEY WORDS

Plant polysaccharide;
Abelmoschus manihot;
Intestinal inflammation;
Mucus barrier;
Interleukin 10;
Gut microbiota;
A. muciniphila;
Mucin 2

Abstract The intestinal mucus barrier is an important line of defense against gut pathogens. Damage to this barrier brings bacteria into close contact with the epithelium, leading to intestinal inflammation. Therefore, its restoration is a promising strategy for alleviating intestinal inflammation. This study showed that *Abelmoschus manihot* polysaccharide (AMP) fortifies the intestinal mucus barrier by increasing mucus production, which plays a crucial role in the AMP-mediated amelioration of colitis. IL-10-deficient mouse models demonstrated that the effect of AMP on mucus production is dependent on IL-10. Moreover, bacterial depletion and replenishment confirmed that the effects of AMP on IL-10 secretion and mucus production were mediated by *Akkermansia muciniphila*. These findings suggest that plant polysaccharides fortify the intestinal mucus barrier by maintaining homeostasis in the gut microbiota. This demonstrates that targeting mucus barrier is a promising strategy for treating intestinal inflammation.

*Corresponding authors.
E-mail addresses: dja@njucm.edu.cn (Jinao Duan), njuguo@njucm.edu.cn (Jianming Guo).
†These authors made equal contributions to this work.

Peer review under the responsibility of Chinese Pharmaceutical Association and Institute of Materia Medica, Chinese Academy of Medical Sciences.

https://doi.org/10.1016/j.apsb.2024.06.002

1. Introduction

The surface of intestinal epithelial cells is covered by a layer of mucus that maintains intestinal homeostasis and protects the intestinal mucosa from potential pathogens[1]. The intestinal mucus layer provides an environment for symbiosis between gut microbes and the host. Gut microbes and the mucus barrier are in dynamic equilibrium in healthy people. In contrast, patients with intestinal inflammation have a thinner intestinal mucus layer[2,3], making it easier for gut microbes to penetrate. Thereafter, gut microbes and their inflammatory products contact the intestinal epithelial cells, consequently triggering the release of proinflammatory cytokines and exacerbating intestinal inflammation[4].

Mucin 2 (MUC2) is a highly glycosylated protein secreted by goblet cells and is a major component of the intestinal mucus layer[5]. *Muc2* deficiency leads to intestinal mucus barrier damage, subsequently inducing spontaneous colitis[6]. In contrast, excess mucus secretion prevents chemical- and microbial-driven intestinal inflammation[7]. This indicates that maintaining intestinal mucus barrier function is a promising strategy for alleviating intestinal inflammation.

Akkermansia muciniphila is an important symbiotic bacterium that is localized to the intestinal mucus layer[8]. It not only grows by degrading MUC2 but also stimulates the secretion of this protein and maintains mucus production[9]. A decrease in *A. muciniphila* may be a hallmark of intestinal inflammation associated with gut microbiota dysbiosis, mucus barrier dysfunction, and immune system overreaction[10,11]. Moreover, supplementation with this bacterium effectively alleviates intestinal inflammation[12].

Chinese medicine comprises natural products of various structural types, such as alkaloids, polysaccharides, flavonoids, and saponins, which have curative effects and low oral bioavailability. The gut microbiota has been used to elucidate the unique mechanisms underlying the curative effects of Chinese medicines[13] such as BaWeiBaiDuSan[14], *Astragali radix*[15], *Panax ginseng* polysaccharide[16], *Morinda officinalis* oligosaccharide[17], *Astragalus* polysaccharide[18,19], *Rabdosia serra*[20], berberine[21–23], and flavones[24].

Abelmoschus manihot, a plant widely distributed throughout eastern Europe and Asia, has high nutritional value for human. However, only a few pharmacological studies have been published on *Abelmoschus manihot* polysaccharide (AMP). Of these, most have focused on its immunomodulatory and anti-tumor activities[25,26]. Thus, the effects of AMP on mucus secretion and the gut microbiota remain unknown. In the present study, AMP alleviated intestinal inflammation by fortifying the intestinal mucus barrier and maintains homeostasis in intestinal *A. muciniphila*. Our findings suggest that herbal polysaccharides can improve the intestinal mucus barrier by maintaining gut microbiota homeostasis. Therefore, targeting the intestinal mucus barrier may be an effective strategy for alleviating intestinal inflammation.

2. Materials and methods

2.1. Drug preparation and administration

Abelmoschus manihot (Linn.) Medicus was provided by Anhui Wansheng Chinese Herbal Pieces Co., Ltd. (Anhui, China). The dried herb was extracted twice with 80% ethanol for 2 h. The residue was extracted twice with water at 100 °C for 2 h. The extracted solutions were concentrated and precipitated by 80% ethanol for 12 h. The precipitate was freeze-dried to obtain AMP.

2.2. AMP molecular weight and monosaccharide composition

AMP was analyzed by high-performance gel permeation chromatography (HPGPC) [PAD; Dionex ICS 5000+ system, TSK-gel G-5000 and 3000 PW, 8.0 mm × 300 mm] and showed two major peaks with molecular weight of 96.4 and 4.6 kDa (Supporting Information Fig. S1A).

The monosaccharide composition was analyzed by Thermo ICS 5000+ ion chromatography system [Dionex™ CarboPac™ PA20, 150 mm × 3.0 mm] using high-performance anion-exchange chromatography (HPAEC). The monosaccharide composition of AMP included 26.31% rhamnose, 29.03% galactose, 5.41% arabinose, 3.4% glucose, 0.73% xylose, 30.8% galacturonic acid, and 4.32% glucuronic acid (Fig. S1B and S1C).

2.3. Animals

Female wild-type C57BL/6J mice of 6–8 weeks old were purchased from Shanghai SLAC Laboratory Animal Co., Ltd. (Shanghai, China), and knockout mice (*Il10*$^{-/-}$, *Muc2*$^{-/-}$) were purchased from GemPharmatech Co., Ltd. (Nanjing, China). All mice were raised in specific-pathogen-free facility. Animal experiments were approved by the Institutional Animal Care and Use Committee of Nanjing University of Chinese Medicine. Mice were provided with *ad libitum* chow and drinking water and maintained on a 12-h light/dark cycle at 24 ± 2 °C and 40%–60% relative humidity. All animal experiments were performed in strict accordance with the regulations of the Animal Ethics Committee of Nanjing University of Chinese Medicine.

2.4. Animal models

DSS-induced acute colitis[27]: For wild-type and *Il10*$^{-/-}$ mice, colitis was induced by administering 2.5% DSS (molecular mass 36,000–50,000 Da; MP Biomedicals, USA) dissolved in drinking water for seven or eight days. In the antibiotic treatment experiment, the susceptibility of mice to DSS was reduced due to the deletion of gut microbiota. Therefore, 3% DSS was used to induce colitis in mice. Mice were sacrificed ten days after DSS cessation.

DSS-induced chronic colitis[27]: Mice were subjected to three cycles of 2.5% DSS in the drinking water for seven days, followed by ten days of recovery. Mice were sacrificed ten days after the last DSS treatment.

Muc2$^{-/-}$induced chronic colitis[6]: *Muc2*$^{-/-}$ mice were raised to two months old to develop chronic colitis.

Disease activity index (DAI) was performed by combining the parameters of weight loss, stool consistency, and rectal bleeding as described. DAI scores were composed of the mean of the total score of the three parameters. DAI scores are shown in Supporting Information Table S1A.

The mice in the control and model groups were administered purified water by oral gavage (0.1 mL per 10 g body weight), and the mice in the AMP-treated group were given AMP (100, 200, and 400 mg/kg).

2.5. Histology

The distal and proximal colon section was collected and fixed in 4% paraformaldehyde, routinely embedded in paraffin, and sliced.

Sections were stained with hematoxylin and eosin (H&E). Histological pathology scores are shown in Table S1B.

The fecal pellets that were wrapped with middle colon tissue, as well as a segment of the proximal and distal colon, were also fixed with Carnoy's solution. For histological staining of mucus and goblet cells, colon tissue sections or mouse fecal sections were immersed in Alcian blue (AB) and Alcian blue/Periodic acid-Schiff (AB/PAS).

Mucus thickness and goblet cells were measured and counted. Five spots per slice were randomly selected for measurement on AB-stained sections. For AB/PAS-stained sections, average goblet cells in 20 crypts were counted per section.

2.6. *Fluorescence in situ hybridization (FISH) of 16S rRNA and mucin staining*

The paraffin sections were de-paraffined and hydrated by reducing the ethanol concentration. The CY3-conjugated-eubacterial 16S rRNA probe hybridization mixture was applied to the tissue. Tissue sections were then incubated at 42 °C overnight. FISH staining was followed by anti-MUC2 antibody. After washing in PBS, the tissue sections were stained with Coralite 488-conjugated goat anti-rabbit IgG (H+L) diluted 1:1000, followed by incubation with DAPI.

2.7. *Flow cytometry analysis*

Mononuclear cells isolated from lamina propria (LP) were stimulated with Cell Activation Cocktail (Biolegend, USA) for 4 h to detect IL-10 secretion. Cells were stained with antibodies for 30 min at 4 °C to identify cell surface antibodies. Intracellular staining was performed using Fixation/Permeabilization Solution (Biolegend, USA), and the cells were fixed for 20 min and stained for IL-10 antibody for 50 min at room temperature. All cells were differentiated with Zombie Yellow™ Fixable Viability Kit (Biolegend, USA). Samples were taken on Gallios flow cytometer (BD Bioscience), and the data were analyzed using Flowjo version 10.8.1. The following antibodies were used for flow cytometry: FITC anti-CD19 (MB19-1, Biolegend), PE/Cyanine7 anti-CD3 (17A2, Biolegend), Alexa Fluor 700 anti-CD45 (S18009F, Biolegend), PE anti-IL-10 (JES5-16E3, BD Biosciences).

2.8. *Bacteria culture*

A. muciniphila (ATCC BAA-835) was obtained from Guangdong Microbial Culture Center (GDMCC, Guangdong, China) and cultured according to *GDMCC* culturing guidelines. *A. muciniphila* was cultured in Brain Heart Infusion (BHI, Solarbio, China) medium, supplemented with 0.2% (*w/v*) of mucin (Yuanye, China) plates and incubated at 37 °C in an anaerobic workstation (DG250, Don Whitley Scientific, UK), that was filled with mixed nitrogen (10% H_2, 10% CO_2, 80% N_2).

For *in vivo* analysis, *A. muciniphila* was cultured overnight, after which the bacteria were centrifuged (7500×*g*, 15 min), resuspended in PBS (1×10^9 CFU/mL), and used as transplant material.

2.9. *16S rRNA gene expression analysis*

Fresh feces were collected before mice were executed, snap-frozen, and shipped to Majorbio Bio-Pharm Technology Co., Ltd. (Shanghai, China) for library preparation, sequencing, and analysis. An Illumina platform was used for DNA pyrosequencing of the V3−V4 hypervariable region of the 16S rRNA gene. Through clustering of operational taxonomic units, species annotation, and abundance analysis, sequencing revealed the species composition of the samples.

2.10. *Statistical analysis*

All data are expressed as means ± standard error of mean (SEM). Unpaired Student's *t*-test, one-way ANOVA, and two-way ANOVA were performed using GraphPad Prism version 8.0 (San Diego, CA, USA). A value of $P < 0.05$ was considered statistically significant.

3. Results

3.1. *AMP alleviated intestinal inflammation and restored the intestinal mucus barrier in acute colitis mice*

To elucidate the effect of AMP on colitis, C57BL/6J mice were administered 2.5% dextran sodium sulfate (DSS) for eight days to construct an acute colitis model. The mice were then orally administered normal saline or different doses of AMP for ten days (Fig. 1A). Mice in the model group suffered from weight loss, diarrhea, and rectal bleeding compared to the control mice, whereas mice in the 400 mg/kg AMP group had less diarrhea and faster weight recovery (Fig. 1B and C; Supporting Information Fig. S2A). AMP (400 mg/kg) also considerably ameliorated colon shortening and splenomegaly in mice with colitis but did not substantially improve the thymus (Fig. 1D; Fig. S2B−S2D). In mice with DSS-induced colitis, the intestinal mucus barrier was impaired, as reflected by its reduced thickness and decreased number of goblet cells in the proximal colon. AMP promoted MUC2 secretion and increased goblet cell number, consequently increasing the thickness of the intestinal mucus layer in a dose-dependent manner (Fig. 1E−J).

Next, we investigated the effects of AMP on intestinal inflammation. Histological assessment of H&E-stained colon sections showed that mice in the DSS group exhibited loss of epithelial crypts, inflammatory cell infiltration, and epithelial damage in the distal colon, whereas 400 mg/kg AMP significantly improved intestinal inflammation (Fig. 1K and L). Moreover, 400 mg/kg AMP downregulated the transcription and expression of the pro-inflammatory cytokines TNF-α and IL-6 (Supporting Information Fig. S3). These results showed that AMP improved intestinal inflammation, with 400 mg/kg showing the best effect. Therefore, we selected 400 mg/kg AMP for the follow-up study.

To investigate whether AMP improves goblet cell function, we evaluated the expression of genes related to endoplasmic reticulum (ER) stress and the *O*-glycosylation of MUC2. AMP markedly affected the expression of the ER stress-related genes *Perk*, *Atf4*, and *Xbp1s* (Fig. 2A). It substantially promoted the expression of the core 3 *O*-glycan genes *B3gnt6*, the core 1 *O*-glycan genes *C1galt1*, and the sialic acid transferase gene *St3gal3*, respectively (Fig. 2B). Although α-1,6-fucosyltransferase (*Fut8*) was not altered in the mouse model, AMP promoted the expression of this gene (Fig. 2B). In addition, MUC5ac is an alternative secreted mucin that is closely associated with colitis progression, with aberrant expression observed during colitis development[28]. However, this model revealed no significant differences in the expression of *Muc5ac* in colon tissue (Fig. 2C).

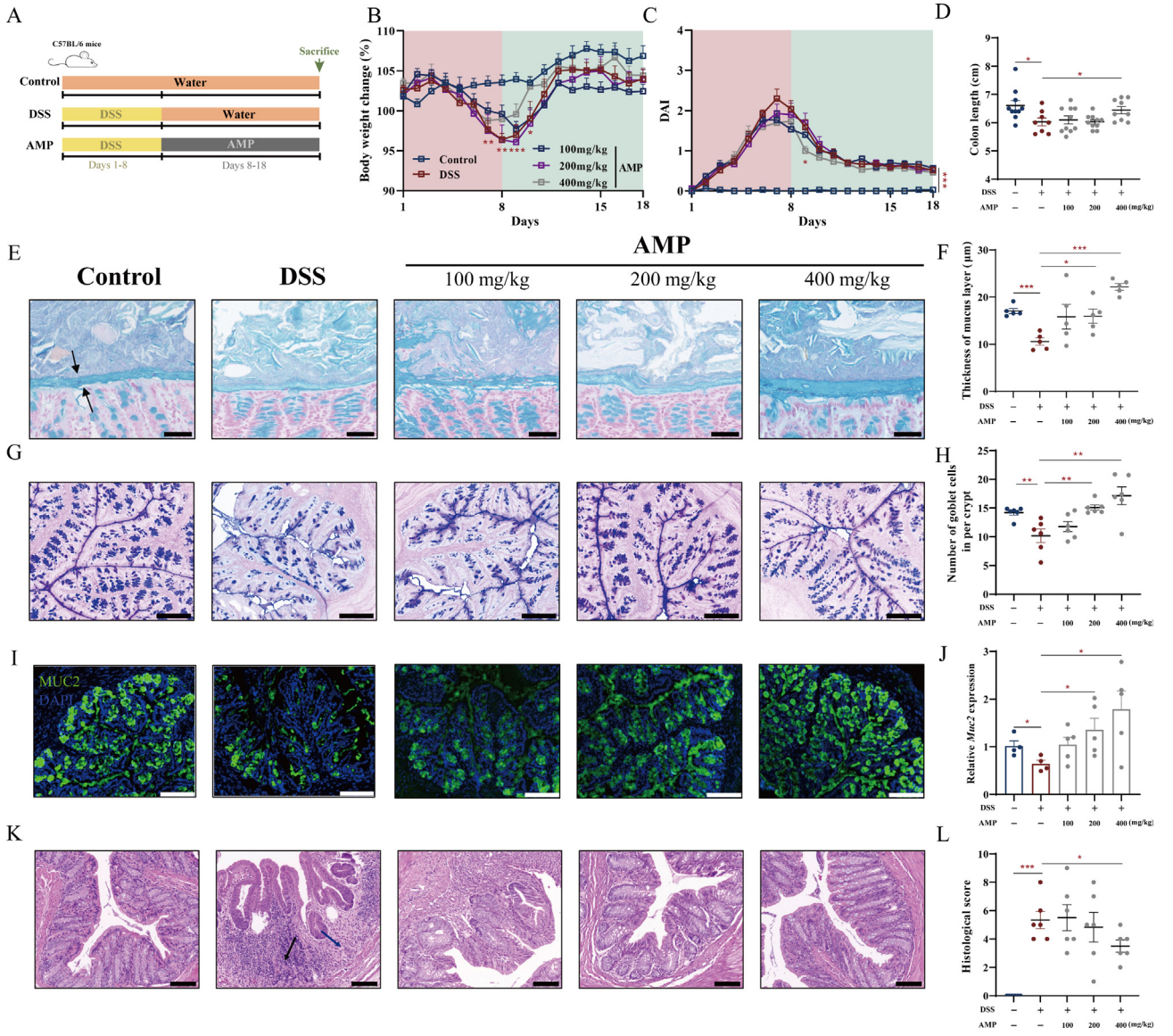

Figure 1 AMP alleviated intestinal inflammation in acute colitis mouse models. (A) C57BL/6 J mice were exposed to 2.5% dextran sodium sulfate (DSS) for eight days, followed by administering different doses of AMP or purified water (DSS, $n = 10$) until being euthanized. Control mice were only administered purified water (Con, $n = 10$). (B) Daily body weight changes after 2.5% DSS administration (*, DSS group compared to Control group). (C) Disease activity index (DAI). (D) Colon lengths ($n = 8-10$). (E) Alcian blue-stained sections of tissues and feces. Images were taken at 40 × magnification (Scale bar: 40 μm, $n = 5$). The arrow indicates the mucus layer. (F) Mucus thickness. (G) Representative pictures showing colon tissues stained with PAS/AB. Images were taken at 20 × magnification (Scale bar: 100 μm, $n = 6$). (H) Numbers of goblet cells in each crypt. (I) Immunostaining for MUC2 (green) in distal colon sections (Scale bar: 100 μm, $n = 3$). (J) *Muc2* expression in colon ($n = 4-5$). (K) Histopathological analysis of distal colonic tissue from mice with acute colitis. Images were taken at 15 × magnification (Scale bar: 100 μm, $n = 6$). The black and blue arrows indicate inflammatory infiltrates and crypt injury, respectively. (L) Histological score. The data are expressed as mean ± SEM, $^*P < 0.05$, $^{**}P < 0.01$, $^{***}P < 0.001$.

Damage to the intestinal mucus layer may lead to microbial invasion into crypts. This reduces the distance between intestinal epithelial cells and gut microbes. This process will trigger intestinal infection and inflammation[29]. Therefore, we investigated the invasion of gut microbes by measuring the distance between the microbes and the surface of intestinal epithelial cells using confocal imaging of Carnoy-fixed colon specimens. DSS markedly reduced the distance between gut microbes and intestinal epithelial cells, and AMP prevented the invasion of gut microbes (Fig. 2D and E). In conclusion, these findings suggest that AMP fortifies the intestinal mucus barrier in mice with DSS-induced colitis.

3.2. AMP improved mucus barrier function in chronic colitis mice

Repeated epithelial damage and wound repair induced by several cycles of DSS administration may cause a non-self-limiting chronic form of colitis. In this study, we investigated the effects of AMP in a mouse model of DSS-induced chronic colitis.

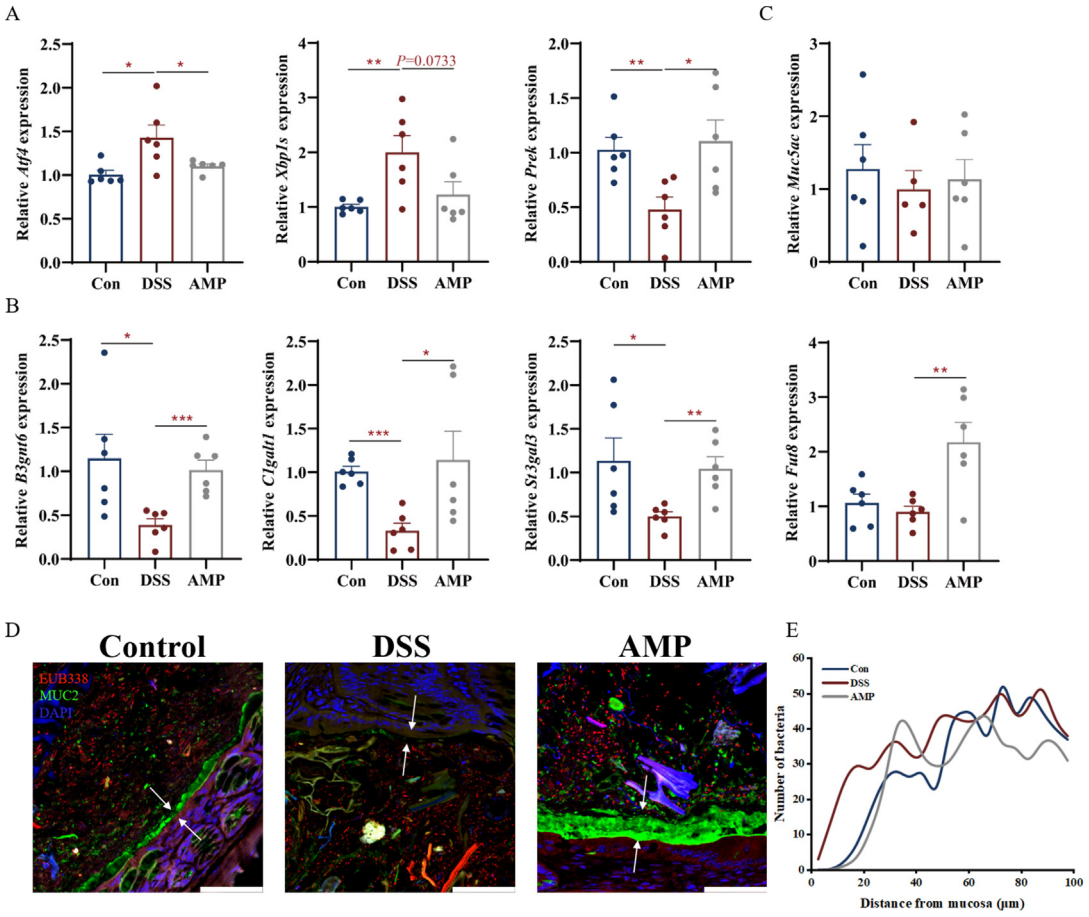

Figure 2 AMP improved mucus barrier function in mice with colitis. (A) The expression of *Atf4*, *Xbp1s*, and *Perk* in colonic tissues was measured using real-time qPCR ($n = 6$). (B) The expression of *B3gnt6*, *C1galt1*, *St3gal3*, and *Fut8* in colonic tissues was measured using real-time qPCR ($n = 6$). (C) *Muc5ac* expression in the colon ($n = 6$). (D) Mucin layer and intestinal bacteria were stained using anti-MUC2 antibody and EUB338 probe. Images were taken at 60 × magnification (Scale bar: 50 μm, $n = 3$). The arrow indicates the mucus layer. (E) The distance between luminal microbiota and epithelial surface. Data are expressed as mean ± SEM, $^{*}P < 0.05$, $^{**}P < 0.01$, $^{***}P < 0.001$.

C57BL/6J mice were administered three cycles of 2.5% DSS through their drinking water. The mice were treated with AMP after every DSS cycle (Fig. 3A). Consistent with the acute colitis model, AMP-treated mice showed reduced susceptibility to DSS-induced chronic colitis, with significant effects on DAI, fecal water content, and colon length compared with control mice (Fig. 3B and C; Supporting Information Fig. S4A). Additionally, AMP improved the histopathology of the distal colon and reduced the transcription of *Tnfa* and *Il6* (Fig. 3D and E; Fig. S4B). These results suggest that AMP ameliorates intestinal inflammation in mice with colitis.

Next, we investigated whether AMP restores intestinal mucus barrier damage in this model. Intestinal mucus secretion was reduced in the model group, whereas AMP markedly restored the thickness of the intestinal mucus (Fig. 3F and G). Consistent with the acute colitis model, AMP prevented the entry of gut microbes into the intestinal epithelial cells (Fig. 3H and I). In addition, we did not observe any adverse effects of AMP on the mouse host (Supporting Information Fig. S5). Our results suggest that AMP restores intestinal mucus barrier function to alleviate acute and chronic colitis.

3.3. Enhanced mucus production played a crucial role in AMP-mediated amelioration of colitis

MUC2 is an essential component of the intestinal mucus layer, and its deficiency leads to intestinal mucus barrier damage, subsequently inducing spontaneous colitis[6]. As AMP restored MUC2 protein and mRNA transcription levels in mice with colitis, we further investigated whether it improves intestinal inflammation by restoring the intestinal mucus barrier. Therefore, *Muc2*$^{-/-}$ mice, which developed diarrhea and rectal bleeding at 6−8 weeks old, were orally administered AMP for 30 days (Fig. 4A).

Muc2$^{-/-}$ mice had lower body weight gain and a more progressive increase in DAI, fecal water content, and colonic atrophy than wild-type mice. Moreover, AMP did not substantially affect this process (Fig. 4B and C; Supporting Information Fig. S6A−S6C). Furthermore, *Muc2*$^{-/-}$ mice exhibited intestinal goblet cell atrophy and thin mucus layers (Fig. 4D and E; Fig. S6D and S6E), leading to inflammatory cell infiltration and pro-inflammatory cytokine secretion (Fig. 4F−H). AMP did not increase the thickness of the intestinal mucus layer and lost its effect on intestinal inflammation in the

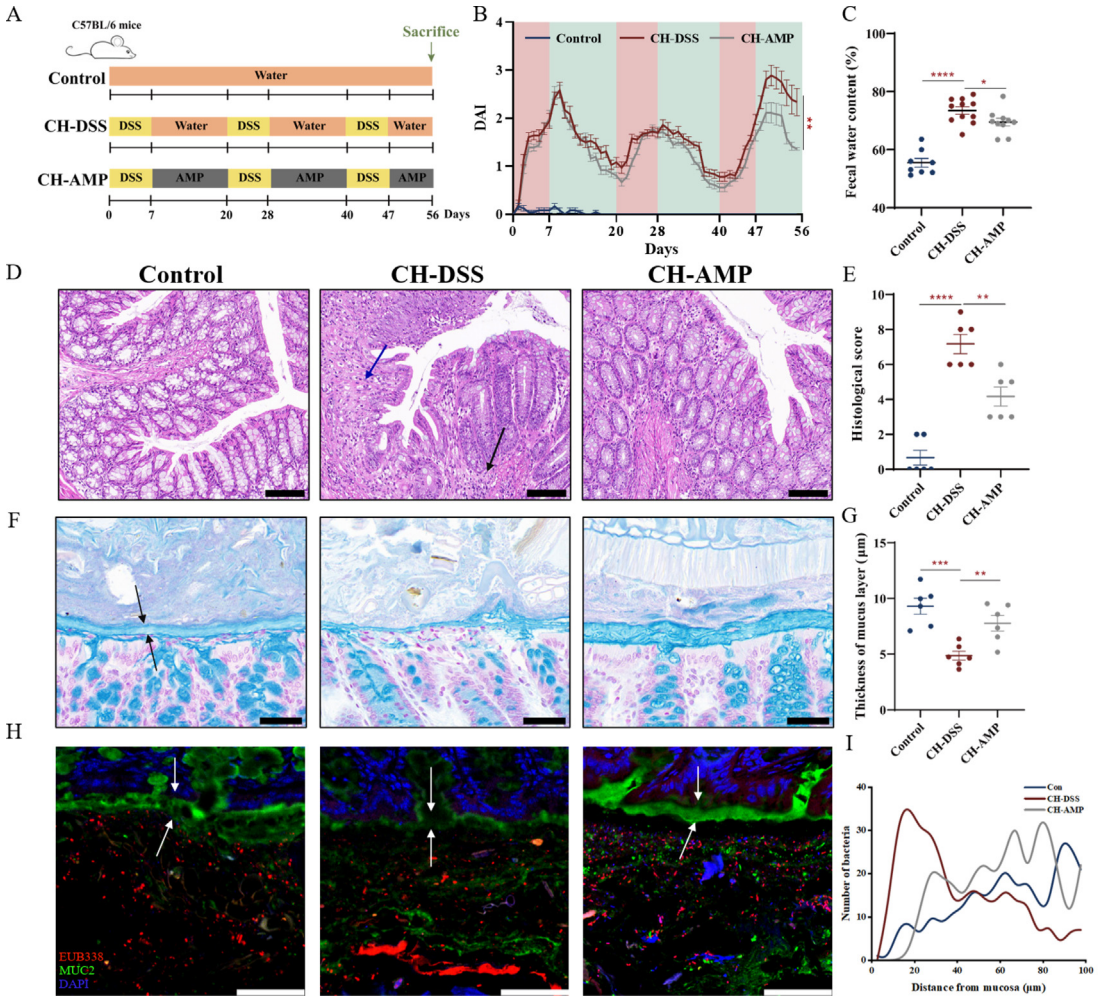

Figure 3 AMP alleviated intestinal inflammation in chronic colitis mice. (A) C57BL/6 J mice were exposed to three cycles of 2.5% DSS in drinking water. These mice were orally administered with AMP (CH-AMP, $n = 12$) or purified water (CH-DSS, $n = 12$) after every cycle of DSS administration until being euthanized. Control mice were only administered purified water (Control, $n = 8$). (B) DAI. (C) Fecal water content ($n = 8-11$). (D) Representative images of the H&E-stained colon sections. Images were captured at 15 × magnification (Scale bar: 100 μm, $n = 6$). Black and blue arrows indicate inflammatory infiltrates and crypt injury, respectively. (E) Histological score. (F) Alcian blue-stained sections of tissues and feces. Images were taken at 40 × magnification (Scale bar: 40 μm, $n = 6$). The arrow indicates the mucus layer. (G) Mucus thickness. (H) Mucin layer and intestinal bacteria following anti-MUC2 antibody and EUB338 probe staining. Images were taken at 60 × magnification (Scale bar: 50 μm, $n = 3$). The arrow indicates the mucus layer. (I) Distance between luminal microbiota and the epithelial surface. Data are expressed as mean ± SEM, $^{*}P < 0.05$, $^{**}P < 0.01$, $^{***}P < 0.001$, $^{****}P < 0.0001$.

absence of *Muc2* (Fig. 4D–H). These findings suggest that enhanced mucus production plays a crucial role in the AMP-mediated amelioration of colitis.

3.4. *The effect of AMP on mucus production was dependent on IL-10 but not on IL-22*

IL-22 is a cytokine that triggers an immune response against gut barrier damage. It improves the destruction of the colitis-associated mucus layer by increasing mucin production[30]. Therefore, we examined *Il22* transcription in mice with colitis. AMP did not have a significant effect on *Il22* transcription in these mice (Supporting Information Fig. S7A), indicating that it does not promote mucus production *via* IL-22.

IL-10 is another crucial anti-inflammatory cytokine that delays the progression of colitis by inhibiting the release of pro-inflammatory cytokines and maintaining the integrity of the intestinal mucus barrier[31]. In the present study, AMP promoted IL-10 secretion in acute and chronic colitis models (Fig. S7B and S7C).

We used $Il10^{-/-}$ mice to evaluate the effect of AMP on mucus production. We induced acute colitis by administering 2.5% DSS to $Il10^{-/-}$ mice for eight days (Fig. 5A). Weight loss, diarrhea, rectal bleeding, and colonic swelling were observed in the $Il10^{-/-}$ mice. However, AMP did not ameliorate these pathological changes (Fig. 5B; Supporting Information Fig. S8A–S8D). AMP lost its ameliorative effect on the intestinal mucus layer (Fig. 5C–G). $Il10^{-/-}$ mice exhibited more severe intestinal inflammation and colonic histopathological damage than wild-type controls. However, AMP did not substantially ameliorate these symptoms (Fig. S8E–S8G). These findings further demonstrate the role of IL-10 in mucus production and AMP-induced amelioration of colitis.

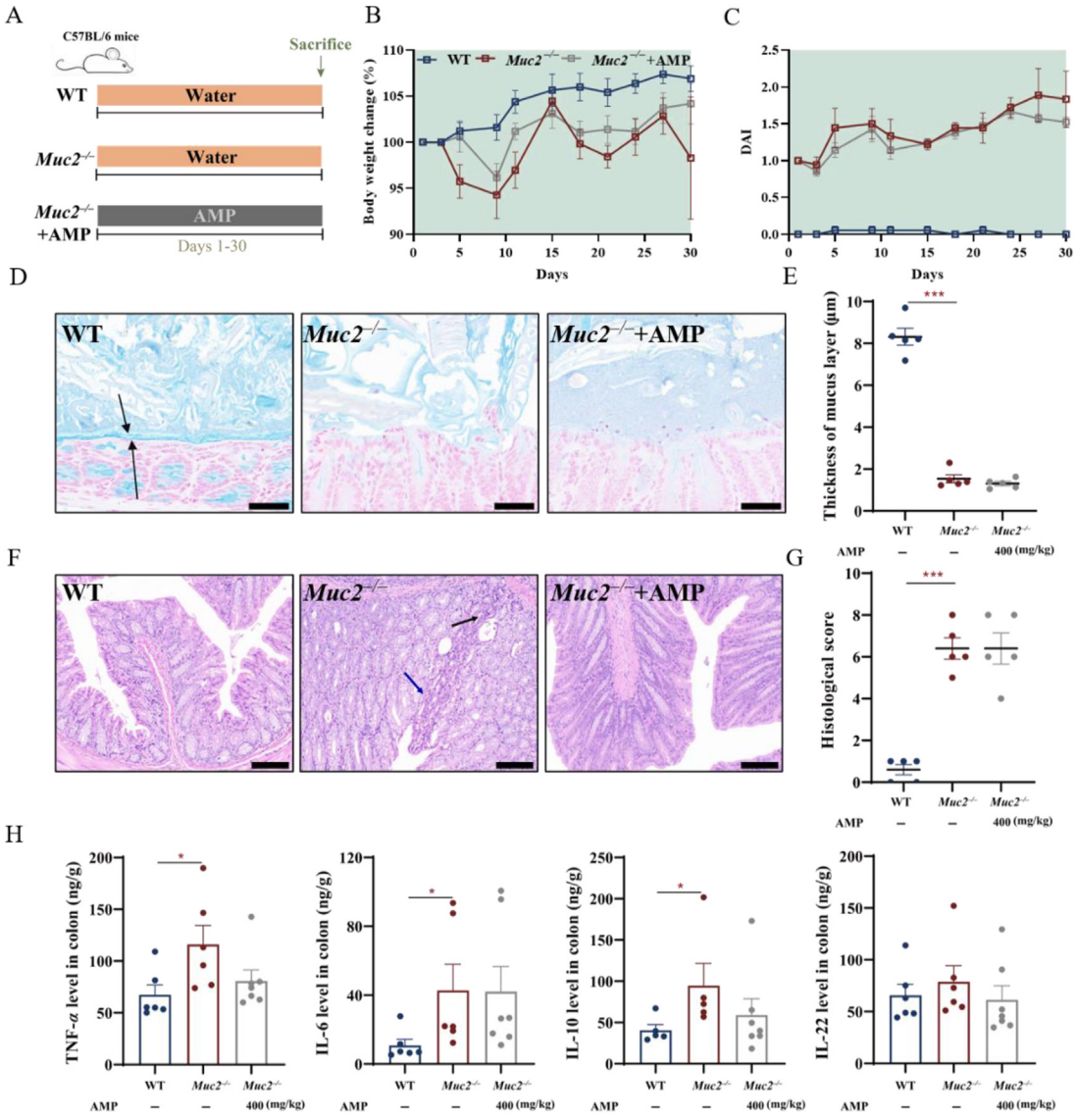

Figure 4 Enhanced mucus production played a crucial role in AMP-mediated amelioration of colitis. (A) Littermate *Muc2*$^{-/-}$ mice were administered daily with AMP (AMP, $n = 6$) or purified water (*Muc2*$^{-/-}$, $n = 7$) for 30 days. Wild-type mice were only administered purified water (WT, $n = 6$). (B) Body weight changes. (C) DAI. (D) Alcian blue-stained sections of tissues and feces. Images were taken at 40 × magnification (Scale bar: 40 μm, $n = 5$). The arrow indicates the mucus layer. (E) Mucus thickness. (F) Histopathological analysis of distal colonic tissue from mice with acute colitis. Images were taken at 15 × magnification (Scale bar: 100 μm, $n = 5$). Black and blue arrows indicate inflammatory infiltrates and crypt injury, respectively. (G) Histological scores. (H) The levels of TNF-α, IL-6, IL-10, and IL-22 expression in the colons of mice ($n = 5$−7). The data are expressed as means ± SEM, $^{*}P < 0.05$, $^{***}P < 0.001$.

To further explore the immune mechanisms mediated by AMP during colitis-induced intestinal injury, we evaluated IL-10-producing immune cells in the colonic lamina propria of DSS-induced acute colitis mice using flow cytometry. IL-10-positive cells were markedly reduced in the colonic lamina propria (Fig. 5H and I). AMP considerably increased the proportion of IL-10-positive T and B cells in the lamina propria (Fig. 5J and K). This suggests that AMP promotes IL-10 secretion by T and B cells in the lamina propria of the colon. These results suggest that AMP improves intestinal inflammation and mucus barrier function in an IL-10-dependent manner.

3.5. AMP improved gut microbiota dysbiosis and increased A. muciniphila abundance

Mounting evidence supports the crucial role of the gut microbiota in mucus production and IL-10 secretion. The intestinal mucus layer provides adhesion sites and nutritional support for the gut microbiota. Thus, damage to the intestinal mucus barrier function can lead to changes in the composition of the gut microbiota[7]. Therefore, we examined alterations in the gut microbiota to further explore whether the effect of AMP on intestinal mucus and IL-10 is associated with the gut microbiota.

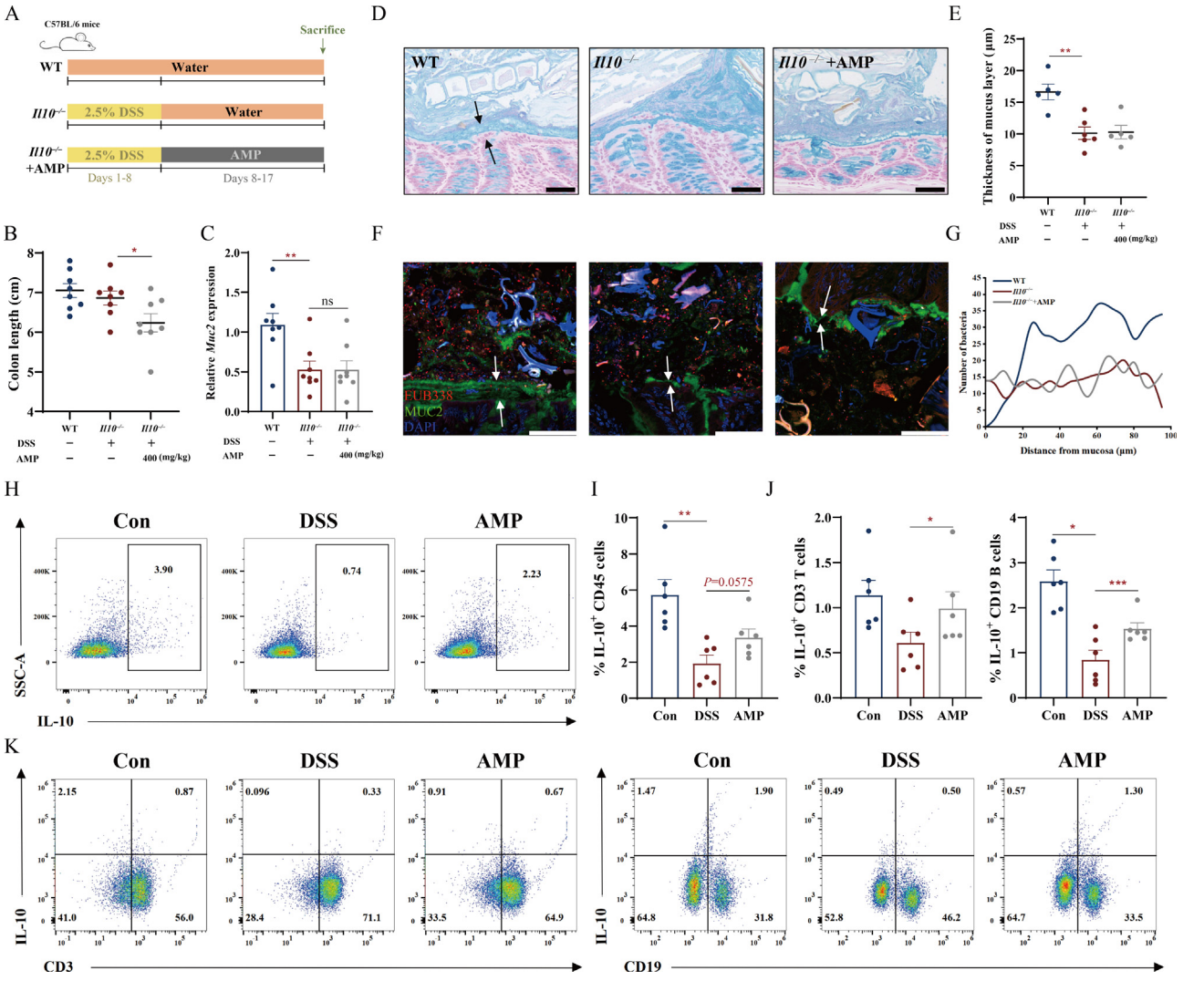

Figure 5 The effect of AMP on mucus production was dependent on IL-10. (A) Littermate *Il10*$^{-/-}$ mice were treated with 2.5% DSS for eight days. The mice were administered daily with AMP (AMP, $n = 8$) or purified water (*Il10*$^{-/-}$, $n = 8$). Wild-type mice were only administered purified water (WT, $n = 8$). (B) Colon lengths ($n = 8$). (C) *Muc2* expression in the colon ($n = 8$). (D) Alcian blue-stained sections of tissues and feces. Images were taken at 40 × magnification (Scale bar: 40 μm, $n = 6$). The arrow indicates the mucus layer. (E) Mucus thickness. (F) The mucin layer and intestinal bacteria following anti-MUC2 antibody and EUB338 probe staining. Images were taken at 60 × magnification (Scale bar: 50 μm, $n = 3$). The arrow indicates the mucus layer. (G) The distance between the luminal microbiota and epithelial surface. (H, I) IL-10 expression in CD45$^+$ cells from the lamina propria of the colon ($n = 6$). (J, K) IL-10 expression in CD3$^+$ T cells and CD19$^+$ B cells from the lamina propria of the colon ($n = 6$). A representative scatter plot and quantitative data are shown. Data are expressed as mean ± SEM, $^*P < 0.05$, $^{**}P < 0.01$, $^{***}P < 0.001$.

We performed high-throughput sequencing of the 16S rRNA from fecal bacterial DNA isolated from mice with acute colitis. The α-diversity of the gut microbiota was markedly reduced after DSS administration. Furthermore, the evenness and diversity of mice in the AMP group were higher than those in the DSS group (Fig. 6A and B). Profiling of the gut microbiota through principal coordinate analysis on Unweighted UniFrac and Bray−Curtis metrics showed significant clustering and separation between groups, with significantly altered fecal microbiota between the control and DSS groups, and AMP reversed this trend (Fig. 6C and D). Relative abundance analysis revealed that bacteria in the phylum Verrucomicrobia were enriched in the AMP group (Fig. 6E). At the genus level, DSS reduced the abundance of *Akkermansia*, *Adlercreutzia*, *Ileibacterium*, and *Monoglobus* and increased that of *Dubosiella*, *Rikenellaceae_RC9_gut_group*, *Romboutsia*, and *Bradyrhizobium* (Supporting Information Fig. S9).

We applied a linear discriminant analysis effect size to identify significant differences in bacterial community dominance in AMP-treated mice. Various microbes, including the mucus-utilizing bacterium *A. muciniphila*, were significantly enriched in AMP-treated mice (Fig. 6F). This finding was confirmed using

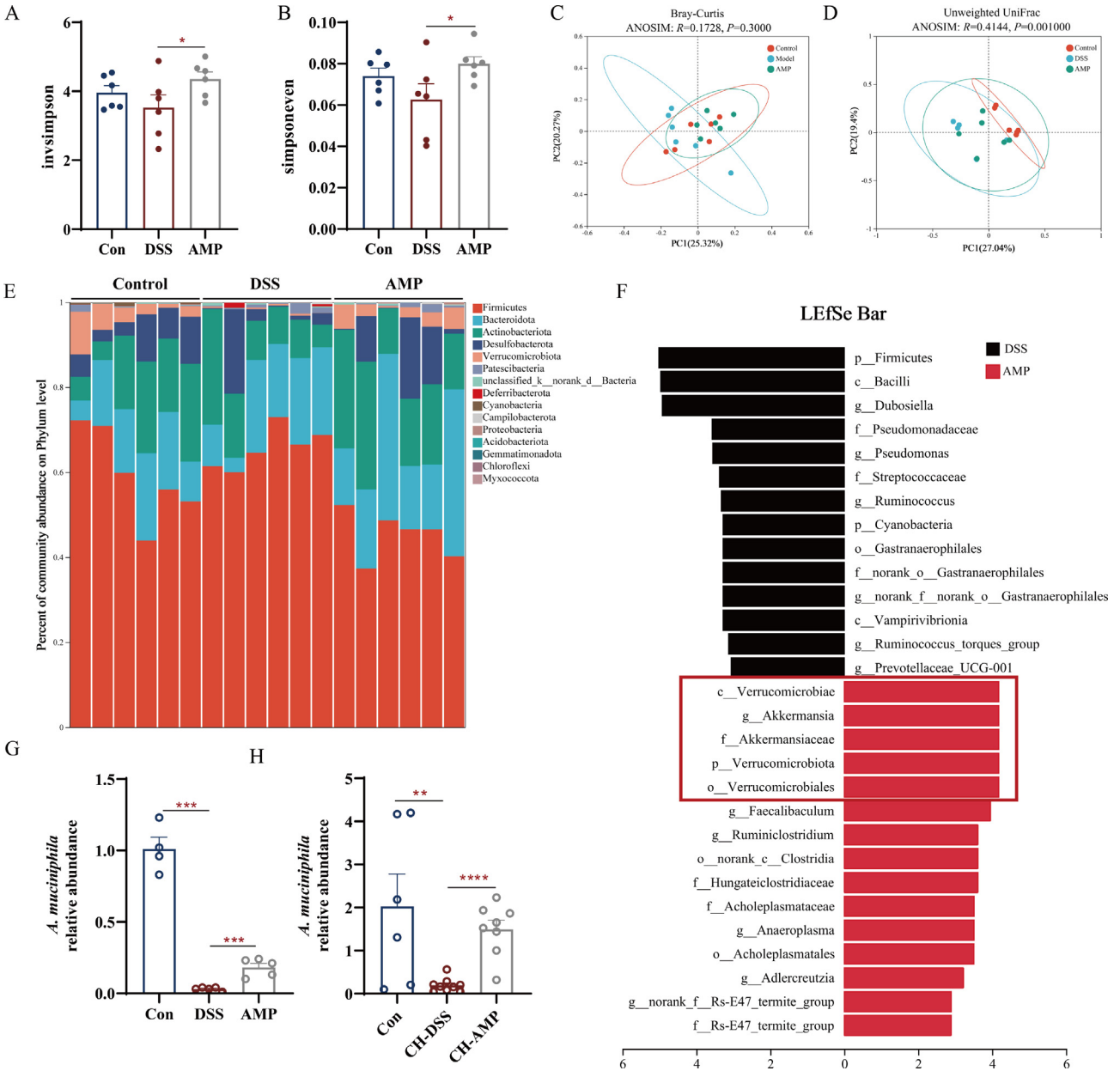

Figure 6 AMP improved gut microbiota dysbiosis and increased *A. muciniphila* abundance. Fecal samples were collected from DSS-induced acute colitis model mice on day 10 of administration, fecal genomic DNA was isolated, and 16S rRNA genes in the V3−V4 region were sequenced. (A, B) Alpha diversity of gut microbiota evenness (simpsoneven index) and diversity (invsimpson index) from different mouse groups. Mann−Whitney test was used to determine statistical significance ($n = 6$). (C, D) Bray−Curtis and Unweighted UniFrac Principal coordinate analysis plot of the beta-diversity of gut microbiota composition in different groups. (E) Taxonomic distributions of gut microbiota composition at the phylum level. (F) Differences in microbial taxa at all taxonomic levels between AMP-treated and DSS-treated mice. The Mann−Whitney test was used, with $P < 0.01$ and LDA score >2.00 considered statistically significant. (G) The relative abundance of *A. muciniphila* in feces from mice with acute colitis was assessed using qPCR ($n = 4$−6). (H) The relative abundance of *A. muciniphila* in feces from mice with chronic colitis was assessed using qPCR ($n = 6$−8). Data are expressed as mean ± SEM, $^*P < 0.05$, $^{**}P < 0.01$, $^{***}P < 0.001$.

qPCR (Fig. 6G). Similarly, *A. muciniphila* abundance was reduced in mice with DSS-induced chronic colitis; AMP significantly restored its abundance (Fig. 6H).

We explored the effects of AMP on bacteria belonging to the Lachnospiraceae and Enterobacteriaceae families. The Lachnospiraceae hydrolyze diet-derived polysaccharides and play a probiotic role in colitis[32], whereas the Enterobacteriaceae proliferate abnormally in patients with colitis and exacerbate intestinal inflammation[33]. However, AMP did not affect the abundance of these bacteria (Supporting Information Fig. S10).

These findings show that this polysaccharide restores homeostasis in the gut microbiota and specifically regulates *A. muciniphila* abundance in mice with colitis.

3.6. The effect of AMP on mucus production and IL-10 secretion was dependent on A. muciniphila

We treated mice with a cocktail of broad-spectrum antibiotics to directly evaluate the role of gut microbes in the effect of AMP on mucus production and IL-10 secretion (Fig. 7A). Two-week antibiotic treatment effectively depleted gut microbes (Supporting Information Fig. S11A−S11D). Colitis was induced using DSS, and then the mice were orally administered normal saline or AMP for ten days (Fig. 7A). Monitoring of water consumption revealed that the groups received comparable amounts of DSS water, suggesting that the therapeutic effect of antibiotics was not due to differences in DSS intake (Fig. S11A and S11B).

Antibiotics reduced the severity of DSS-induced colitis compared to non-antibiotic-treated controls, as evidenced by improvements in body weight, diarrhea, rectal bleeding, visceral index, mesenteric lymph node weight, and colon length (Supporting Information Fig. S12). Similarly, the production of pro-inflammatory cytokines was reduced in antibiotic-treated mice (Fig. 7B). Owing to the therapeutic effect of antibiotics in mice with colitis, the administration of AMP after antibiotic treatment did not improve inflammation-related parameters. Therefore, we cannot confirm whether AMP ameliorates inflammation-related indicators in mice with colitis after the clearance of the gut microbiota.

Although antibiotics protect mice with colitis from inflammation, antibiotic treatment did not repair intestinal mucus barrier damage in this study. *Muc2* transcription (Fig. 7B) and mucus thickness were reduced, and proximal colonic goblet cells were damaged in the model group. However, antibiotics did not have a therapeutic effect (Fig. 7C−F). Furthermore, *Il10* transcription was reduced after antibiotic treatment, and AMP could not reverse this trend (Fig. 7B). AMP did not protect the intestinal mucus barrier (Fig. 7C−F), suggesting that its effect on mucus production and IL-10 secretion is dependent on the gut microbiota. These results indicate that AMP repairs the intestinal mucus barrier by modulating the gut microbiota in mice with colitis.

Our study showed that AMP substantially regulates the abundance of *A. muciniphila* in acute and chronic colitis. *A. muciniphila* abundance decreased sharply after broad-spectrum antibiotic treatment, and AMP did not restore it (Fig. S11E). *A. muciniphila* ameliorates intestinal inflammation and promotes intestinal mucus secretion in DSS-induced acute colitis[10]. Therefore, we hypothesized that AMP may improve intestinal mucus barrier function by regulating *A. muciniphila* abundance. To test this hypothesis, we inoculated wild-type mice with *A. muciniphila* *via* oral gavage and administered AMP after inoculation (Fig. 7G).

Compared to the *A. muciniphila* group, gavage of *A. muciniphila* followed by AMP administration considerably restored weight loss, diarrhea, rectal bleeding, and the shortened colon length in mice with acute colitis (Supporting Information Fig. S13). MUC2 protein and mRNA transcription levels were significantly higher in AMP-treated mice than in *A. muciniphila*-treated controls (Fig. 7H and I). In addition, the gavage of *A. muciniphila*, followed by AMP administration, markedly increased the thickness of the intestinal mucus layer (Fig. 7J and K). Although AMP-induced promotion of IL-10 was lost following gut microbial deletion, this effect was restored after colonization with *A. muciniphila* (Fig. 7B and L).

These findings demonstrate that *A. muciniphila* plays a key role in the effects of AMP on mucus production and IL-10 secretion. However, the mechanism by which AMP works through *A. muciniphila* remains unclear.

3.7. The effect of AMP on A. muciniphila was not mediated by MUC2 and IL-18

In this study, AMP restored *A. muciniphila* abundance in DSS-induced acute and chronic colitis. The intestinal mucus provides nutrients for *A. muciniphila* growth; thus, mucus production facilitates *A. muciniphila* colonization. Therefore, we hypothesized that AMP restores *A. muciniphila* abundance by promoting mucus secretion, and that *A. muciniphila* feeds back into the intestinal mucus layer, ultimately thickening this layer and forming a positive feedback loop. However, analysis of the gut microbes of *Muc2*$^{-/-}$ mice revealed that AMP considerably promotes *A. muciniphila* proliferation (Supporting Information Fig. S14A), suggesting that the effect of AMP on *A. muciniphila* was not mediated by mucus.

Other factors that regulate *A. muciniphila* abundance include IL-18, a cytokine that stimulates T cell-mediated IFN-γ production[34]. The abundance of *A. muciniphila* increased significantly in *Il18*$^{-/-}$ mice and recombinant IL-18 administration reduced *A. muciniphila* colonization in *Nlrp6*$^{-/-}$ mice[35]. We evaluated *Il18* transcription in mice with DSS-induced acute colitis to investigate whether AMP promotes *A. muciniphila* proliferation by modulating IL-18 secretion. AMP did not inhibit *Il18* transcription in this study (Fig. S14B), suggesting that the promotion of *A. muciniphila* growth by AMP was not mediated by IL-18.

As AMP promotes *A. muciniphila* growth in a way unrelated to the pathways mentioned above, we hypothesized that AMP directly promotes *A. muciniphila* growth.

3.8. AMP directly promoted A. muciniphila growth by upregulating the expression of microbial genes and regulating cell growth and energy metabolism

Bacteria were cultured *in vitro* to further elucidate the effects of AMP on *A. muciniphila*. AMP promoted bacterial growth (Fig. 8A) in the BHI medium supplemented with mucin. Moreover, *A. muciniphila* grew slowly in the absence of mucin in the BHI medium but grew faster in AMP-containing media (Fig. 8B).

Next, we used RNA-sequencing on AMP-treated *A. muciniphila* to investigate changes in microbial gene expression. The quality and quantity of sequencing data demonstrate the accuracy and reproducibility of our RNA-Seq results (Supporting Information Tables S2 and S3). Principal component analysis revealed significant differences between the control and AMP groups, indicating that *A. muciniphila* function changes globally (Fig. 8C; Supporting Information Table S4). In total, 64 differentially expressed genes (DEGs) were found between the two groups. Of these, the expression of 40 genes mainly related to cell growth and energy metabolism was upregulated in the AMP group (Fig. 8D).

Cluster of orthologous gene (COG) enrichment analysis was performed on the DEGs to elucidate their biological function, with significant functional differences between upregulated and downregulated genes. The COG functions enriched in the genes

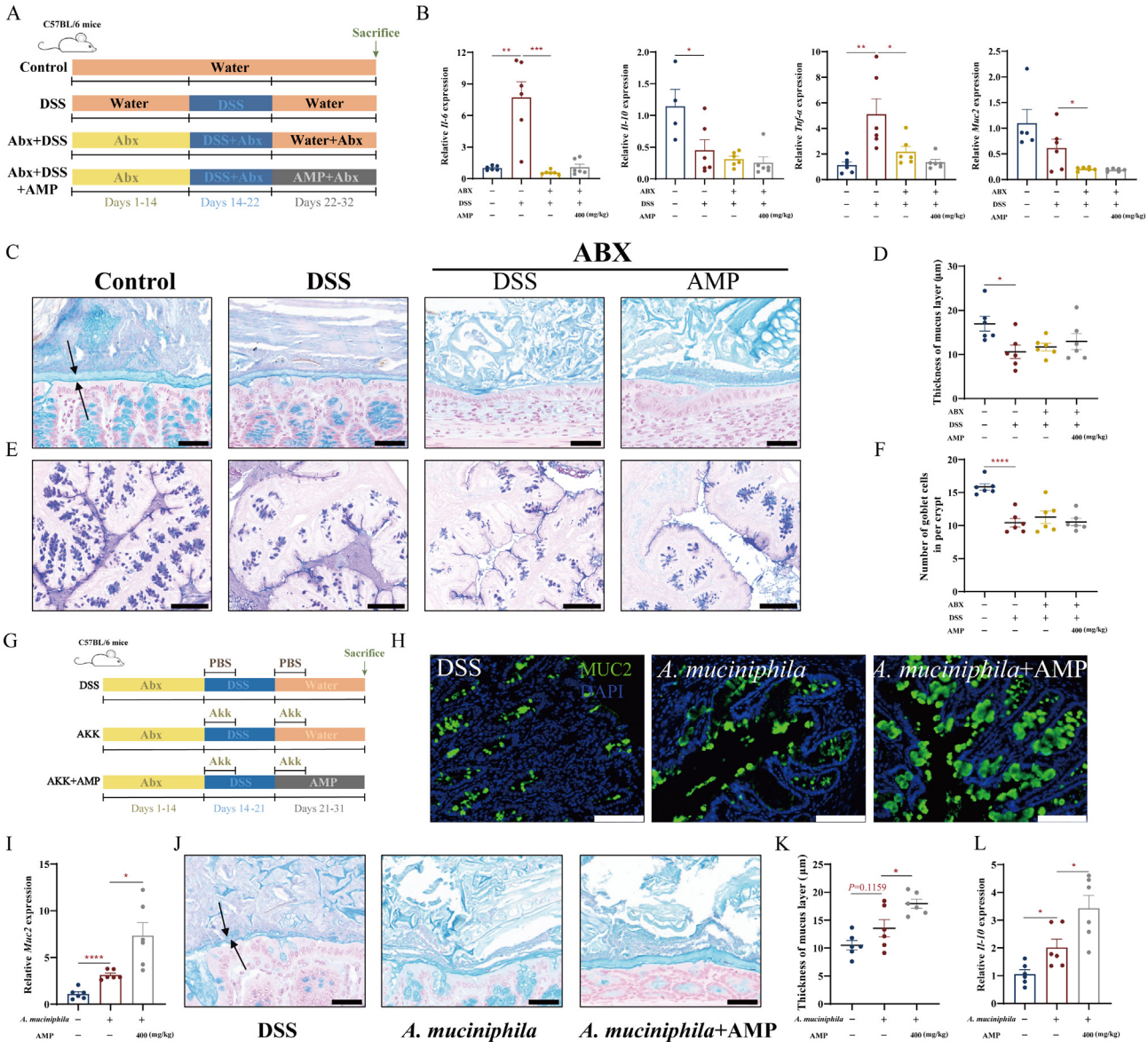

Figure 7 The effect of AMP on mucus production and IL-10 secretion was dependent on *A. muciniphila*. (A) C57BL/6 J mice were randomly divided into the control, DSS, and Abx-treated groups ($n = 8-10$ per group). The control group was given purified water throughout the process, and the DSS group was operated the same way as the DSS + Abx group, except that no Abx was administered. The Abx-treated mice were administered Abx in drinking water for two weeks and subsequently exposed to 3% DSS for eight days to deplete the gut microbiota. At the end of the DSS exposure, these mice were administered with AMP or purified water for ten days. During DSS and AMP treatment, mice were treated with Abx until euthanasia. (B) Intestinal RNA levels of inflammatory cytokines (*Tnfα*, *Il10*, and *Il6*) and *Muc2* in mice ($n = 4-6$). (C) Alcian blue-stained sections of tissues and feces. Images were taken at 40 × magnification (Scale bar: 40 μm, $n = 6$). The arrow indicates the mucus layer. (D) Mucus thickness. (E) Representative images of the PAS/AB staining of proximal colon sections of different treatment groups. Images were taken at 20 × magnification (Scale bar: 100 μm, $n = 6$). (F) Numbers of goblet cells in each crypt. (G) C57BL/6J mice ($n = 6-10$ per group) were fed with Abx in drinking water for two weeks and subsequently exposed to 3% DSS. These mice were administered with *A. muciniphila*, AMP plus *A. muciniphila*, or purified water. (H) MUC2 immunofluorescence staining of distal colon tissue (Scale bar: 100 μm, $n = 3$). (I) *Muc2* expression in the colon ($n = 6$). (J) Alcian blue-stained sections of tissues and feces. Images were taken at 40 × magnification (Scale bar: 40 μm, $n = 6$). The arrow indicates the mucus layer. (K) Mucus thickness. (L) *Il10* expression in the colon ($n = 6$). Data are expressed as mean ± SEM, $^{*}P < 0.05$, $^{**}P < 0.01$, $^{***}P < 0.001$, $^{****}P < 0.0001$.

whose expression was upregulated included cell wall, membrane, and envelope biogenesis; translation; carbohydrate transport; and metabolism. These genes were indicators of increased bacterial growth (Fig. 8E). The transcriptomic data indicated that the expression of genes associated with carbohydrate metabolism was upregulated in the AMP group (Supporting Information Fig. S15).

Gene ontology terms enriched among the genes whose expression was upregulated included ATP hydrolysis activity (GO:0016887) and carbohydrate transport (GO:0008643). Moreover, Kyoto Encyclopedia of Genes and Genomes pathway enrichment analysis showed that the citrate cycle (map00020) was significantly enriched (Supporting Information Table S5). These

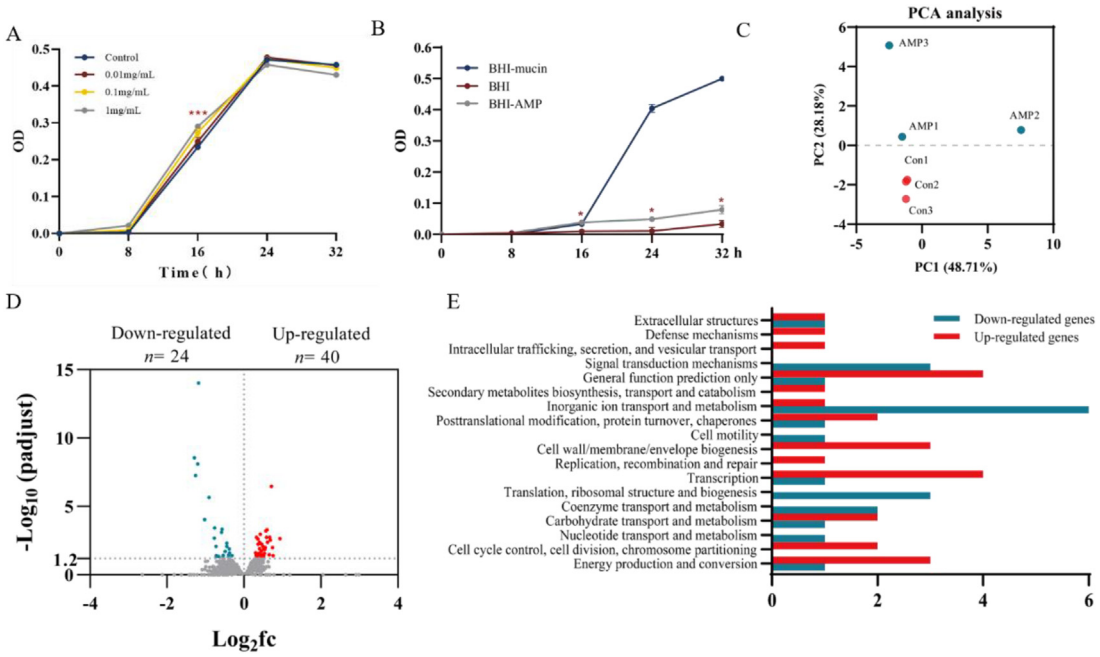

Figure 8 AMP directly promoted *A. muciniphila* growth by upregulating the expression of microbial genes that regulate cell growth and energy metabolism. (A) Growth curves showing the effects of different concentrations of AMP on *A. muciniphila*. (B) Growth curves showing the action of AMP on *A. muciniphila* in the mucin-free medium. (C) Scatter plot of principal component analysis. (D) Volcano plot of genes sequenced under Control and AMP conditions. (E) COG annotations of DEGs among DEGs whose expression was upregulated (red) and downregulated (blue). Data are expressed as mean ± SEM, $n = 3$ for each group. $^{*}P < 0.05$, $^{***}P < 0.001$.

results suggest that AMP directly promotes *A. muciniphila* growth by regulating microbial genes.

4. Discussion

The 2019 consensus guidelines on the management of IBD, published by the British Society of Gastroenterology, recognized herbal remedies as complementary and alternative therapies for adults with IBD[36]. Polysaccharides are common natural active ingredients in herbal medicines and have a wide range of bioactivities such as anti-oxidative stress[37], anti-inflammatory[38], and lipid-modulating effects. Additionally, they have received extensive attention as potential therapeutic agents for IBD. The present study revealed that AMP mainly comprises galactose, rhamnose, arabinose, galacturonic acid, and glucuronic acid. Among these monosaccharides, galactose, arabinose, and rhamnose are closely associated with the immunological activity of polysaccharides.

The gut microbiota maintains intestinal homeostasis and activates the host immune system. Sellon et al.[39] reported that *Il10*$^{-/-}$ mice raised in a conventional SPF environment developed IBD, whereas those raised in a germ-free environment did not exhibit signs of intestinal inflammation. This indicates that the development of intestinal inflammation requires the gut microbiota. Therefore, research targeting the gut microbiota for treating intestinal inflammation has made considerable progress. Clinical studies have demonstrated the efficacy of probiotics and fecal transplantation in alleviating clinical symptoms and reducing inflammation in patients with IBD[40-42]. Herbal medicines can inhibit intestinal mucosal inflammation in patients with IBD by modulating the gut microbiota, restoring intestinal mucosal immune balance and exerting therapeutic effects against IBD. This suggests that herbal medicine could be a promising therapeutic strategy for treating IBD, as it regulates the gut microbiota[43,44]. In the present study, our microbial analyses showed that AMP restored gut microbiota homeostasis and modulated *A. muciniphila* abundance in mice with colitis.

A. muciniphila penetrates and interacts with the intestinal mucus layer to maintain homeostasis. Moreover, the intestinal mucus barrier function is closely associated with various intestinal inflammatory diseases, such as intestinal infections, IBD, and colorectal cancer[45-47]. Inflammation in the colon is often accompanied by damage to the mucus barrier function, which leads to increased intestinal permeability and consequent inflammatory damage to the intestinal epithelial cells[48]. Restoration of intestinal mucus barrier function by herbal polysaccharides has been reported. *Ganoderma lucidum* polysaccharide[49], *Serratula chinensis* polysaccharide[50], and *Eucommia ulmoides* polysaccharide-modified SeNP[51] promoted MUC2 secretion and increased the number of goblet cells in a mouse model of colitis. However, the specific pathways and mechanisms by which herbal polysaccharides promote MUC2 secretion remain unknown. Our study elucidated the mechanism through which AMP improves the intestinal mucus barrier function.

The present study demonstrated that AMP alleviates intestinal mucus barrier damage in DSS-induced acute and chronic colitis mice. AMP could not restore intestinal mucus barrier function and lost its effect on intestinal inflammation in the absence of *Muc2*. It

indicates that AMP does not directly exert anti-inflammatory effects but acts by restoring intestinal mucus barrier function.

IL-10 is primarily secreted by T cells, B cells, DCs, and macrophages and is a pleiotropic cytokine with potent anti-inflammatory properties[52]. It helps MUC2 folding by upregulating the expression of genes involved in this process and ER stress in adverse conditions of goblet cells[53], which maintain the mucus barrier and prevent inflammation by sustaining MUC2 production and secretion. When IL-10 signaling was inhibited, mice developed more severe ER and goblet cell dysfunction[53].

We found that IL-10 secretion was increased in *Muc2*$^{-/-}$ mice, which has also been reported previously[54]. The authors found that both pro- and anti-inflammatory immune responses were activated in the intestines of *Muc2*$^{-/-}$ mice. Based on the close correlation between IL-10 and MUC2, we proposed that as *Muc2*$^{-/-}$ mice manifested thinner mucus barrier and colon inflammation, *Muc2*$^{-/-}$ mice using a compensatory mechanism to promote IL-10 secretion, which may facilitate proper folding of other mucins, alleviate colon inflammation and maintain low-grade inflammation in the absence of MUC2.

Based on the current study, it could be proposed that promoting intestinal IL-10 secretion to facilitate proper MUC2 folding may be an effective strategy for restoring the intestinal mucus barrier in colitis. *A. muciniphila* promoted IL-10 secretion in a previous study[55]. The present study showed that AMP promoted IL-10 secretion from intestinal immune cells by increasing *A. muciniphila* abundance in mice with colitis, which regulated MUC2 secretion, improved the intestinal mucus barrier, and exerted a therapeutic effect on colitis.

To our knowledge, this study is the first to report the specific mechanism through which plant polysaccharides fortify the intestinal mucus barrier and to prove that *A. muciniphila* plays a vital role in this effect. Our study showed that AMP, a plant polysaccharide, fortifies the intestinal mucus barrier by maintaining gut microbiota homeostasis. Our findings prove that targeting the intestinal mucus barrier is a promising strategy for treating intestinal inflammation.

5. Conclusions

Our study demonstrated that AMP promoted IL-10 secretion by restoring *A. muciniphila* abundance in mice with colitis, thereby promoting MUC2 secretion, improving intestinal mucus barrier function, and ultimately ameliorating intestinal inflammation in mice with colitis.

Acknowledgments

This research was supported by the National Natural Science Foundation of China (82074136), High level key discipline construction project of the National Administration of Traditional Chinese Medicine-Resource Chemistry of Chinese Medicinal Materials (No. zyyzdxk-2023083, China).

Author contributions

Yumeng Wang: Writing − review & editing, Writing − original draft, Visualization, Validation, Methodology, Formal analysis, Data curation, Conceptualization. Chengxi Li: Validation, Methodology, Data curation. Jianping Li: Methodology, Formal analysis, Data curation. Shu Zhang: Formal analysis, Data curation. Qinyu Zhang: Visualization. Jinao Duan: Supervision, Project administration. Jianming Guo: Writing − review & editing, Writing − original draft, Supervision, Project administration, Funding acquisition, Conceptualization.

Conflicts of interest

The authors declare that there is no conflict of interest.

Appendix A. Supporting information

Supporting information to this article can be found online at https://doi.org/10.1016/j.apsb.2024.06.002.

References

1. Birchenough GMH, Johansson MEV. Forming a mucus barrier along the colon. *Science* 2020;**370**:402−3.
2. Johansson ME, Gustafsson JK, Holmén-Larsson J, Jabbar KS, Xia L, Xu H, et al. Bacteria penetrate the normally impenetrable inner colon mucus layer in both murine colitis models and patients with ulcerative colitis. *Gut* 2014;**63**:281−91.
3. van der Post S, Jabbar KS, Birchenough G, Arike L, Akhtar N, Sjovall H, et al. Structural weakening of the colonic mucus barrier is an early event in ulcerative colitis pathogenesis. *Gut* 2019;**68**:2142−51.
4. Okumura R, Takeda K. Roles of intestinal epithelial cells in the maintenance of gut homeostasis. *Exp Mol Med* 2017;**49**:e338.
5. Nyström EEL, Martinez-Abad B, Arike L, Birchenough GMH, Nonnecke EB, Castillo PA, et al. An intercrypt subpopulation of goblet cells is essential for colonic mucus barrier function. *Science* 2021;**372**:eabb1590.
6. Van der Sluis M, De Koning BA, De Bruijn AC, Velcich A, Meijerink JP, Van Goudoever JB, et al. Muc2-deficient mice spontaneously develop colitis, indicating that MUC2 is critical for colonic protection. *Gastroenterology* 2006;**131**:117−29.
7. Naama M, Telpaz S, Awad A, Ben-Simon S, Harshuk-Shabso S, Modilevsky S, et al. Autophagy controls mucus secretion from intestinal goblet cells by alleviating ER stress. *Cell Host Microbe* 2023;**31**:433−46.e4.
8. Yan J, Sheng L, Li H. Akkermansia muciniphila: is it the holy grail for ameliorating metabolic diseases? *Gut Microbes* 2021;**13**:1984104.
9. Zheng M, Han R, Yuan Y, Xing Y, Zhang W, Sun Z, et al. The role of *Akkermansia muciniphila* in inflammatory bowel disease: current knowledge and perspectives. *Front Immunol* 2022;**13**:1089600.
10. Qu S, Fan L, Qi Y, Xu C, Hu Y, Chen S, et al. *Akkermansia muciniphila* alleviates dextran sulfate sodium (DSS)-induced acute colitis by NLRP3 activation. *Microbiol Spectr* 2021;**9**:e0073021.
11. Ma J, Liu Z, Gao X, Bao Y, Hong Y, He X, et al. Gut microbiota remodeling improves natural aging-related disorders through *Akkermansia muciniphila* and its derived acetic acid. *Pharmacol Res* 2023;**189**:106687.
12. Wang L, Tang L, Feng Y, Zhao S, Han M, Zhang C, et al. A purified membrane protein from *Akkermansia muciniphila* or the pasteurised bacterium blunts colitis associated tumourigenesis by modulation of $CD8^+$ T cells in mice. *Gut* 2020;**69**:1988−97.
13. Yang Y, Wang Y, Zhao L, Wang F, Li M, Wang Q, et al. Chinese herbal medicines for treating ulcerative colitis *via* regulating gut microbiota-intestinal immunity axis. *Chin Herb Med* 2023;**15**:181−200.
14. Fan X, Mai C, Zuo L, Huang J, Xie C, Jiang Z, et al. Herbal formula BaWeiBaiDuSan alleviates polymicrobial sepsis-induced liver injury via increasing the gut microbiota *Lactobacillus johnsonii* and regulating macrophage anti-inflammatory activity in mice. *Acta Pharm Sin B* 2023;**13**:1164−79.

15. Li T, Gao X, Yan Z, Wai TS, Yang W, Chen J, et al. Understanding the tonifying and the detoxifying properties of Chinese medicines from their impacts on gut microbiota and host metabolism: a case study with four medicinal herbs in experimental colitis rat model. *Chin Med* 2022;**17**:118.
16. Huang J, Liu D, Wang Y, Liu L, Li J, Yuan J, et al. Ginseng polysaccharides alter the gut microbiota and kynurenine/tryptophan ratio, potentiating the antitumour effect of antiprogrammed cell death 1/programmed cell death ligand 1 (anti-PD-1/PD-L1) immunotherapy. *Gut* 2022;**71**:734−45.
17. Zhang ZW, Gao CS, Zhang H, Yang J, Wang YP, Pan LB, et al. Morinda officinalis oligosaccharides increase serotonin in the brain and ameliorate depression *via* promoting 5-hydroxytryptophan production in the gut microbiota. *Acta Pharm Sin B* 2022;**12**:3298−312.
18. Zheng N, Wang H, Zhu W, Li Y, Li H. Astragalus polysaccharide attenuates nonalcoholic fatty liver disease through THDCA in high-fat diet-fed mice. *J Ethnopharmacol* 2024;**320**:117401.
19. Ma J, Hong Y, Zheng N, Xie G, Lyu Y, Gu Y, et al. Gut microbiota remodeling reverses aging-associated inflammation and dysregulation of systemic bile acid homeostasis in mice sex-specifically. *Gut Microbes* 2020;**11**:1450−74.
20. Li H, Wang Y, Shao S, Yu H, Wang D, Li C, et al. Rabdosia serra alleviates dextran sulfate sodium salt-induced colitis in mice through anti-inflammation, regulating Th17/Treg balance, maintaining intestinal barrier integrity, and modulating gut microbiota. *J Pharm Anal* 2022;**12**:824−38.
21. Ma SR, Tong Q, Lin Y, Pan LB, Fu J, Peng R, et al. Berberine treats atherosclerosis *via* a vitamine-like effect down-regulating choline-TMA-TMAO production pathway in gut microbiota. *Signal Transduct Tar* 2022;**7**:207.
22. Pan L, Yu H, Fu J, Hu J, Xu H, Zhang Z, et al. Berberine ameliorates chronic kidney disease through inhibiting the production of gut-derived uremic toxins in the gut microbiota. *Acta Pharm Sin B* 2023;**13**:1537−53.
23. Wang Y, Tong Q, Ma SR, Zhao ZX, Pan LB, Cong L, et al. Oral berberine improves brain dopa/dopamine levels to ameliorate Parkinson's disease by regulating gut microbiota. *Signal Transduct Tar* 2021;**6**:77.
24. Wang P, Wu R, Jia Y, Tang P, Wei B, Zhang Q, et al. Inhibition and structure-activity relationship of dietary flavones against three loop 1-type human gut microbial β-glucuronidases. *Int J Biol Macromol* 2022;**220**:1532−44.
25. Zheng X, Liu Z, Li S, Wang L, Lv J, Li J, et al. Identification and characterization of a cytotoxic polysaccharide from the flower of *Abelmoschus manihot*. *Int J Biol Macromol* 2016;**82**:284−90.
26. Luan F, Wu Q, Yang Y, Lv H, Liu D, Gan Z, et al. Traditional uses, chemical constituents, biological properties, clinical settings, and toxicities of *Abelmoschus manihot* L.: a comprehensive review. *Front Pharmacol* 2020;**11**:1068.
27. Wirtz S, Popp V, Kindermann M, Gerlach K, Weigmann B, Fichtner-Feigl S, et al. Chemically induced mouse models of acute and chronic intestinal inflammation. *Nat Protoc* 2017;**12**:1295−309.
28. Olli KE, Rapp C, O'Connell L, Collins CB, McNamee EN, Jensen O, et al. Muc5ac expression protects the colonic barrier in experimental colitis. *Inflamm Bowel Dis* 2020;**26**:1353−67.
29. Zou J, Chassaing B, Singh V, Pellizzon M, Ricci M, Fythe MD, et al. Fiber-mediated nourishment of gut microbiota protects against diet-induced obesity by restoring IL-22-mediated colonic health. *Cell Host Microbe* 2018;**23**:41−53.e4.
30. Sugimoto K, Ogawa A, Mizoguchi E, Shimomura Y, Andoh A, Bhan AK, et al. IL-22 ameliorates intestinal inflammation in a mouse model of ulcerative colitis. *J Clin Invest* 2008;**118**:534−44.
31. Neumann C, Scheffold A, Rutz S. Functions and regulation of T cell-derived interleukin-10. *Semin Immunol* 2019;**44**:101344.
32. Sun D, Bai R, Zhou W, Yao Z, Liu Y, Tang S, et al. Angiogenin maintains gut microbe homeostasis by balancing α-Proteobacteria and Lachnospiraceae. *Gut* 2021;**70**:666−76.
33. Zhu W, Winter MG, Byndloss MX, Spiga L, Duerkop BA, Hughes ER, et al. Precision editing of the gut microbiota ameliorates colitis. *Nature* 2018;**553**:208−11.
34. Sivakumar PV, Westrich GM, Kanaly S, Garka K, Born TL, Derry JM, et al. Interleukin 18 is a primary mediator of the inflammation associated with dextran sulphate sodium induced colitis: blocking interleukin 18 attenuates intestinal damage. *Gut* 2002;**50**:812−20.
35. Seregin SS, Golovchenko N, Schaf B, Chen J, Pudlo NA, Mitchell J, et al. NLRP6 protects *Il10*$^{-/-}$ mice from colitis by limiting colonization of *Akkermansia muciniphila*. *Cel Rep* 2017;**19**:733−45.
36. Lamb CA, Kennedy NA, Raine T, Hendy PA, Smith PJ, Limdi JK, et al. British society of gastroenterology consensus guidelines on the management of inflammatory bowel disease in adults. *Gut* 2019;**68**:s1−106.
37. Yuan Q, Yuan Y, Zheng Y, Sheng R, Liu L, Xie F, et al. Anti-cerebral ischemia reperfusion injury of polysaccharides: a review of the mechanisms. *Biomed Pharmacother* 2021;**137**:111303.
38. Yuan D, Li C, Huang Q, Fu X, Dong H. Current advances in the anti-inflammatory effects and mechanisms of natural polysaccharides. *Crit Rev Food Sci* 2023;**63**:5890−910.
39. Sellon RK, Tonkonogy S, Schultz M, Dieleman LA, Grenther W, Balish E, et al. Resident enteric bacteria are necessary for development of spontaneous colitis and immune system activation in interleukin-10-deficient mice. *Infect Immun* 1998;**66**:5224−31.
40. Weingarden AR, Vaughn BP. Intestinal microbiota, fecal microbiota transplantation, and inflammatory bowel disease. *Gut Microbes* 2017;**8**:238−52.
41. Liu CY, Polk DB. Microbiomes through the looking glass: what do UC? *Cell Host Microbe* 2018;**24**:472−4.
42. Cheifetz AS, Gianotti R, Luber R, Gibson PR. Complementary and alternative medicines used by patients with inflammatory bowel diseases. *Gastroenterology* 2017;**152**. 415-29.e15.
43. Zhao L, Zhang S, He P. Mechanistic understanding of herbal therapy in inflammatory bowel disease. *Curr Pharm Des.* 2017;**23**:5173−9.
44. Yu H, Xu H, Yang X, Zhang Z, Hu J, Lu J, et al. Gut microbiota-based pharmacokinetic-pharmacodynamic study and molecular mechanism of specnuezhenide in the treatment of colorectal cancer targeting carboxylesterase. *J Pharm Anal* 2023;**13**:1024−40.
45. Martens EC, Neumann M, Desai MS. Interactions of commensal and pathogenic microorganisms with the intestinal mucosal barrier. *Nat Rev Microbiol* 2018;**16**:457−70.
46. Fang J, Wang H, Zhou Y, Zhang H, Zhou H, Zhang X. Slimy partners: the mucus barrier and gut microbiome in ulcerative colitis. *Exp Mol Med* 2021;**53**:772−87.
47. Pothuraju R, Chaudhary S, Rachagani S, Kaur S, Roy HK, Bouvet M, et al. Mucins, gut microbiota, and postbiotics role in colorectal cancer. *Gut Microbes* 2021;**13**:1974795.
48. Johansson ME, Hansson GC. Immunological aspects of intestinal mucus and mucins. *Nat Rev Immunol* 2016;**16**:639−49.
49. Guo C, Guo D, Fang L, Sang T, Wu J, Guo C, et al. *Ganoderma lucidum* polysaccharide modulates gut microbiota and immune cell function to inhibit inflammation and tumorigenesis in colon. *Carbohyd Polym* 2021;**267**:118231.
50. Li Z, Wen Q, Pi J, Zhang D, Nie J, Wei W, et al. An inulin-type fructan isolated from *Serratula chinensis* alleviated the dextran sulfate sodium-induced colitis in mice through regulation of intestinal barrier and gut microbiota. *Carbohyd Polym* 2023;**320**:121206.
51. Ye R, Guo Q, Huang J, Wang Z, Chen Y, Dong Y. Eucommia ulmoides polysaccharide modified nano-selenium effectively alleviated DSS-induced colitis through enhancing intestinal mucosal

barrier function and antioxidant capacity. *J Nanobiotechnol* 2023; **21**:222.
52. Saraiva M, O'Garra A. The regulation of IL-10 production by immune cells. *Nat Rev Immunol* 2010;**10**:170−81.
53. Hasnain SZ, Tauro S, Das I, Tong H, Chen AC, Jeffery PL, et al. IL-10 promotes production of intestinal mucus by suppressing protein misfolding and endoplasmic reticulum stress in goblet cells. *Gastroenterology* 2013;**144:**357-68.e9.
54. Borisova MA, Achasova KM, Morozova KN, Andreyeva EN, Litvinova EA, Ogienko AA, et al. Mucin-2 knockout is a model of intercellular junction defects, mitochondrial damage and ATP depletion in the intestinal epithelium. *Sci Rep* 2020;**10**:21135.
55. Hänninen A, Toivonen R, Pöysti S, Belzer C, Plovier H, Ouwerkerk JP, et al. *Akkermansia muciniphila* induces gut microbiota remodelling and controls islet autoimmunity in NOD mice. *Gut* 2018; **67**:1445−53.